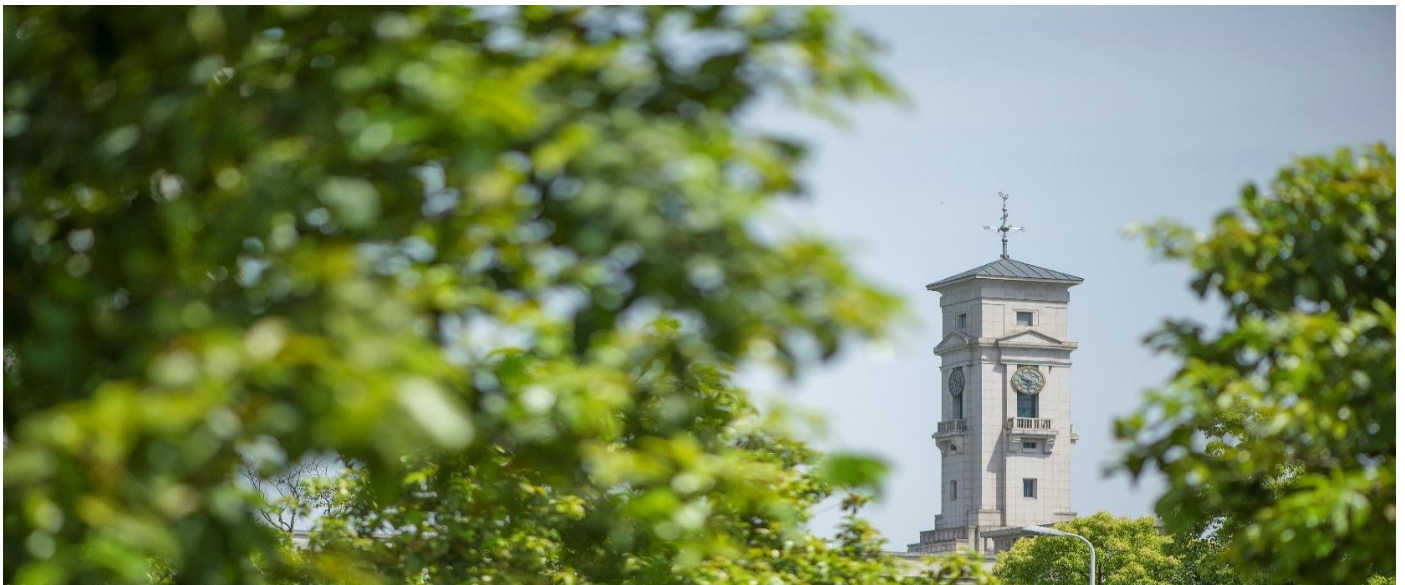


Comparison of slotted and slotless PM machines for high kW/kg aerospace applications

Nisarg Dave, Gaurang Vakil, Zeyuan Xu, Chris Gerada, He Zhang, and David Gerada



**University of
Nottingham**

UK | CHINA | MALAYSIA

University of Nottingham Ningbo China, 199 Taikang East Road, Ningbo,
315100, China

First published 2020

This work is made available under the terms of the Creative Commons
Attribution 4.0 International License:

<http://creativecommons.org/licenses/by/4.0>

The work is licenced to the University of Nottingham Ningbo China
under the Global University Publication Licence:

[https://www.nottingham.edu.cn/en/library/documents/research-
support/global-university-publications-licence.pdf](https://www.nottingham.edu.cn/en/library/documents/research-support/global-university-publications-licence.pdf)



**University of
Nottingham**

UK | CHINA | MALAYSIA

Comparison of slotted and slotless PM machines for high kW/kg aerospace applications

Nisarg Dave^{1,2}, Gaurang Vakil¹, Zeyuan Xu¹, Chris Gerada¹, He Zhang², and David Gerada¹

¹ PEMC Group, University of Nottingham, United Kingdom

² PEMC Group, University of Nottingham Ningbo, China

Abstract — With the ambitious targeted emissions reduction, the aircraft industry is moving towards drastically different aircraft architectures including hybrid-electric. These in turn require electrical machines with a step change improvement in power-density (kW/kg). This paper explores the potential of slotless surface permanent magnet (PM) machines for aerospace applications and compares the predicted power density (kW/kg) of slotless machines to their slotted counterparts.

Index Terms — High power density, slotless machine, airgap winding, permanent magnet machine.

I. INTRODUCTION

Permanent magnet (PM) machines are widely adopted in many transport applications due to their superior power density. Power density can be classified as volumetric [kW/L], as well as gravimetric [kW/kg]. For the next generation hybrid-electric aircraft, often system architects do not have specific volumetric constraints, however the feasibility of an aircraft concept is critically dependent on maximizing the electrical machine's power-to-mass ratio [kW/kg]. Within the hybrid-electric aircraft both the generators as well as the propulsion motors operate at a fairly constant speed, and in the sub-10MW range surface PM machines give the highest gravimetric power densities.

Most of the studies to date focused on improving the power density of slotted surface PM machines. In [1] a comprehensive kW/kg study is made considering slotted surface PM machines, and in [2] the detailed design of a slotted inner rotor surface PM machine is described for aircraft propulsion. This paper extends the work carried out in [1] to include kW/kg comparison between slotted and slotless configurations. The previous research [1] has shown that the majority of the active mass (>60%) is in the stator electrical steel, hence by adopting a slotless topology this component of active mass is markedly reduced. On the other hand, slotless machines have higher flux leakage due to the long effective airgap.

This paper describes a tool for finding the most power dense design of slotless motor for aircraft propulsion. The results of which is compared with the existing slotted machine design to give the idea for comparison. Starting with the 4-pole machine the search has been

carried out up to 40-pole machine with distributed windings. For each coil-pole combination the optimization has been run for 20 A/mm² and 30 A/mm² of current density. For this study inner rotor construction has been considered. The validity of the tool is done by FEA software and results are shown in the discussion. Finally, the most optimal design is identified out of many designs and the validation and comparison has been carried out for that design.

Section II talks about already available state-of-the-art slotted machine for propulsion application of power density of 5-6 kW/kg. Section III focuses on slotless machine, key formulation for electromagnetic design. Section IV talks on discovering the most optimal design. In this section result of the optimization is done and discussion on it is presented. The no-load and on-load results of analytical optimization and FEA of selected design has been shown in this section. Finally, the conclusion has been set up in section V.

II. EXISTING SOA MACHINES

The aerospace industry is aiming for mass minimization over volume minimization. Many researchers are working toward achieving higher kW/kg. Siemens motor for light electric aircraft shows the power density of 5.2 kW/kg [7]. The power node for the developed Siemens motor is 260kW, 2500rpm.

Also, another motor from [2], developed an prototype of electric aircraft propulsion motor using optimization of the problem and by incorporating electromagnetic, thermal and mechanical performance. The motor has demonstrated power density over 5kW/kg. The power node for this motor is same as the research presented in this paper i.e. 500kW, 3000rpm. The slot-pole combination of the motor is 30-poles and 36-slots. The prototype presented in [2] has concentrated windings. Analysis shows that maximum power density can be achieved by using distributed windings with 1 slot per pole per phase. Hence in this paper, the study has been focused for slotless machine with single layer winding and 1 coil side per pole per phase. The study in this paper focuses on to develop an electromagnetically optimized and power dense motor for similar power and speed (500kW, 3000rpm) using slotless architecture.

III. ELECTROMAGNETIC CALCULATION

The slotless construction usually features Halbach magnetized permanent magnets. This is due to flux-concentration characteristic of the Halbach magnets, near sinusoidal airgap flux and lesser requirement of the rotor yoke. The analytical modeling of the Halbach rotor has been performed by several researchers. One of this study has been presented in [3]. Paper [4] discuss about different magnetization pattern of permanent magnet for slotless motor. Out of which the n-stage Halbach rotor is used for discussed application. For this paper, the distributed winding slotless topology has been selected. The copper fill factor is assumed 0.6 throughout the paper.

A. Halbach Array Permanent Magnet

The Halbach array achieves nearly sinusoidal airgap magnetic field by n-stage Halbach array. By using multiple pre-magnetized PM segment with different direction, sinusoidal airgap field can be achieved. Also, by using ferro magnetic or non-magnetic material as a rotor back iron the airgap field is not much affected compared to uniform or radial magnets. Thus, further weight of the machine can be reduced by incorporating this advantage of Halbach magnet. In this application and optimization 5-stage Halbach magnet is used. The air gap magnetic field B_g can be calculated from [3]. The magnet material used here is Recoma 35E. Fig. 1 shows the Halbach magnetized rotor for 6-pole machine with ferro magnetic back iron of rotor.

$$B(\theta, t) = \sum_{n=1}^{\infty} B_{gn} \cos(np\theta - n\omega t) \quad (1)$$

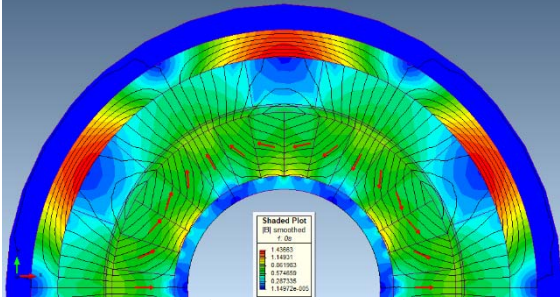


Fig. 1 5-Stage Halbach magnetized rotor with rotor back iron

B. Slotless Windings:

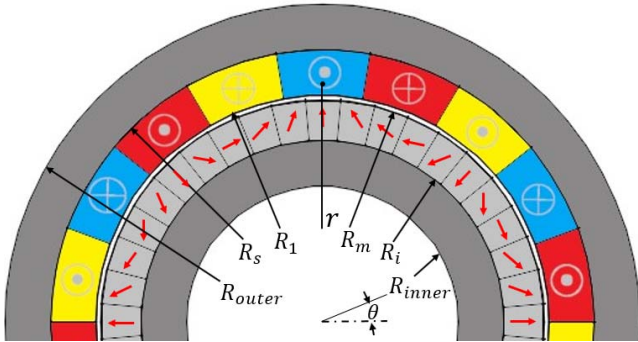


Fig. 2 Nomenclature for inner rotor slotless distributed winding motor

For this paper overlapping winding, i.e. distributed winding is considered for the given application. For overlapping winding the space between two coil sides of one coil is occupied by other two phases. The end winding length is also higher than that of non-overlapping or concentrated winding.

The flux-linkage in one phase can be calculated as flux in one coil into number of turns. Paper [5] talks about winding analysis of distributed winding and equation for flux linkage and back emf can be written as (2) and (3).

$$\psi(t) = \frac{2LB_{g1}R_wN_c k_p}{a} \cos(\theta_0 - \omega t) \quad (2)$$

$$e(t) = \frac{2LB_{g1}R_wN_c k_p \omega}{a} \sin(\theta_0 - \omega t) \quad (3)$$

Here, L is the axial length of the machine, B_{g1} is the maximum amplitude of the fundamental air-gap field due to magnets. N_c is the number of turns per coil, θ_0 is initial geometrical phase shift between stator axis and rotor axis. ω is angular velocity and t being time in seconds and a is number of parallel paths in the winding. R_w and pitch factor k_p is given by following equations.

$$R_w = \frac{R_1 + R_s}{2} \quad (4)$$

$$k_p = \frac{\sin(y_q/2q)}{(y_q/2q)} \quad (5)$$

Where, y_q is one coil side pitch in electrical degree, given as, $y_q = \pi p/C$ and q is slot per pole per phase. And C is number of coils in the machine.

Simultaneously, from [6] the average electromagnetic torque for overlapping winding can be obtained as,

$$T_{avg} = 3B_{g1}pLR_w k_p N_c I_m \quad (6)$$

Here, p is the number of pole pairs. Current density is also one important factor while considering the sizing of the machine. Thermal performance, losses and torque are dependent on the current density of the machine. The equation of current density can be written as,

$$J = \frac{2I_m N_c C}{\pi(R_s^2 - R_1^2)k_{fill}} \quad (7)$$

Here, k_{fill} is the fill factor of the coil. The stator back iron can be calculated using following formula.

$$h_{ys} = \frac{B_{g1}\tau_p}{2B_{ys}} \quad (8)$$

Here, τ_p is pole pitch $\tau_p = \pi R_1/p$ and B_{ys} is saturation limit of the stator yoke steel i.e. around 2T.

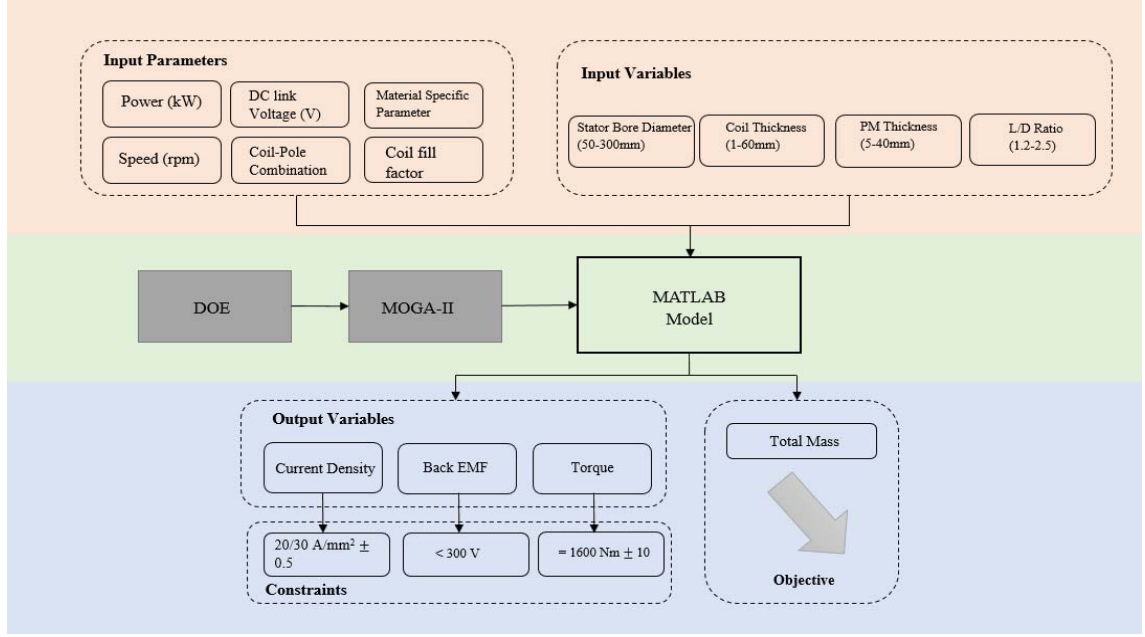


Fig. 3 modeFrontier electromagnetic domain optimization model for 500kW, 3000 rpm nested optimization process

C. Mass Calculation:

Mass calculation is one important parameter for obtaining power density of the machine. In slotless machine, the active mass corresponds to mass of windings, magnet mass and stator and rotor back iron mass. The calculation of mass is shown in the equations below.

$$Mass_{yoke} = \rho_{steel}(Vol_{stator} + Vol_{rotor}) \quad (9)$$

$$Mass_{magnet} = \rho_{magnet}(Vol_{magnet}) \quad (10)$$

$$Mass_{copper} = \rho_{copper}(Vol_{copper} + Vol_{EW}) \quad (11)$$

Here, ρ_{steel} , ρ_{magnet} , and ρ_{copper} are the mass density of steel, magnet and copper material used respectively.

$$Vol_{stator} = \pi L(R_{outer}^2 - R_s^2) \quad (12)$$

$$Vol_{rotor} = \pi L(R_i^2 - R_{inner}^2) \quad (13)$$

$$Vol_{magnet} = \pi L(R_m^2 - R_i^2) \quad (14)$$

$$Vol_{copper} = \pi L(R_s^2 - R_i^2)k_{fill} \quad (15)$$

$$Vol_{EW} = \pi^2 R_e R_{ab}^2 C k_{fill} / 2 \quad (16)$$

Here, $R_{ab} = \pi R_w / C$ and $R_e = \alpha / 2$. Where $\alpha = R_w \theta$ and $\theta = 3\pi / C$ for distributed windings. The active mass is the summation of all these masses.

$$Mass_{Active} = Mass_{yoke} + Mass_{magnet} + Mass_{copper} \quad (17)$$

IV. OPTIMIZATION AND RESULTS

An GA-based design environment is used to determine the power-density of the slotless surface-PM topology, shown in Fig.2. A 5-stage Halbach array is selected in order to achieve the high fundamental airgap flux density, while reducing the harmonic content. The GA-based environment is shown in Fig 3. Essentially it consists of three levels. In the top level (peach-colored) the geometric parameters which can describe any machine variant (4-input variable in the case of slotless SPM) are included. In the second level (green-colored), the calculator scripts are included. Basically, these scripts evaluate the performance of an arbitrary machine geometry in achieving the target power/speed, calculate the current density, back emf and torque as well as estimate the total mass. The third level (blue-colored) sets the constraints for a design to be valid (example: phase back emf < 300V), together with the goals of the optimization (single objective, to minimize the total mass).

For optimization process, starting from 6-coils, 4-pole machine the optimization has been run up to 60-coils, 40-poles machine with distributed winding, power 500kW, speed 3000 rpm and, copper fill factor 0.6. For each pole number, 20,000 different designs were evaluated for highest power density of slotless machine. From the given constraints, the pareto-front has been generated and the optimal design is selected for each coil-pole combination for 20A/mm² and 30 A/mm² current density. There are three constraints for generating the valid designs. The first constraint is current density limit, second constraint is of maximum phase back emf limit i.e. 300V and third constraint is torque, which should be 1600 ± 10 Nm. The input parameters and variables are as shown in Fig.3. from this search space the optimal designs are generated and selected.

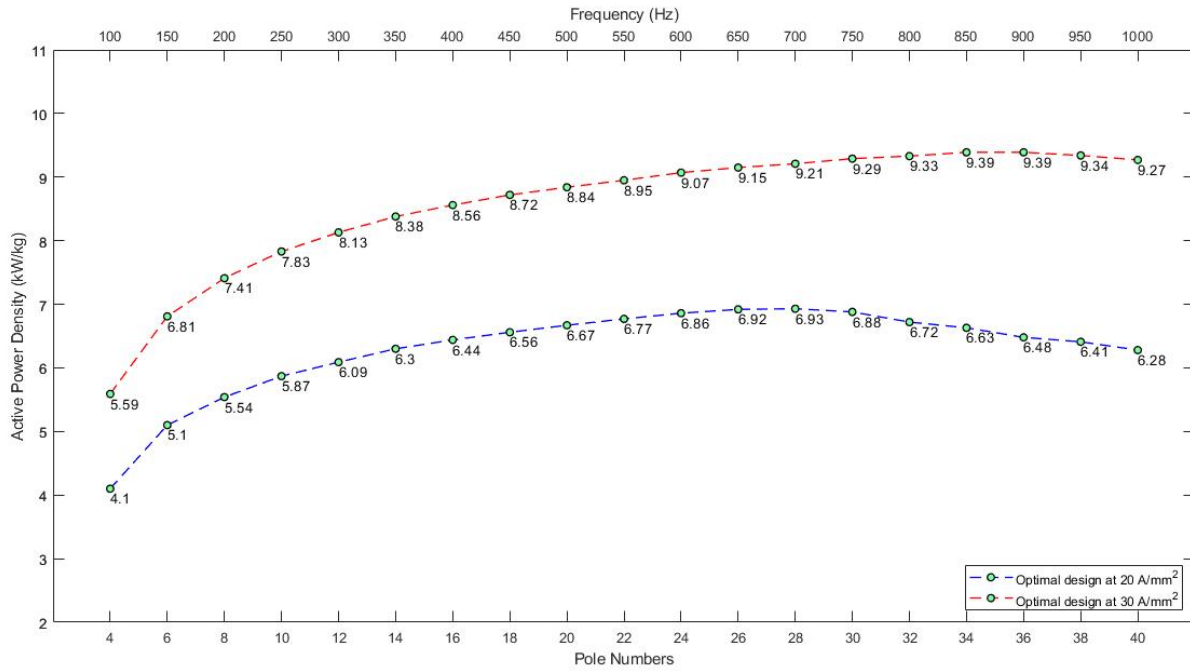


Fig. 4 Optimal design at each slot-pole combination, active power density vs pole number

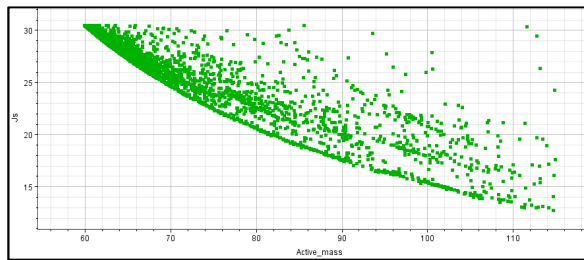


Fig. 5 Pareto-Front for 12-Coils, 8-Poles slotless machine at 30A/mm²

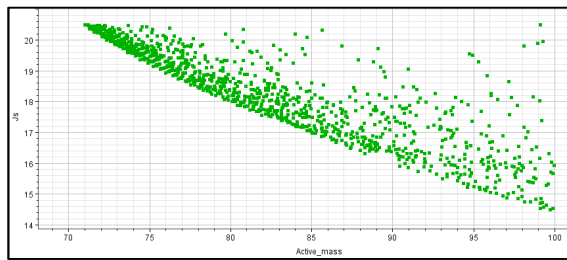


Fig. 6 Pareto-Front for 42-Coils, 28-Poles slotless machine at 20 A/mm²

From the optimization of 40 different designs, two pareto-front of current density vs. active mass has been shown in Fig. 5 and Fig.6. The left-hand side of designs in the pareto-front gives the most optimal design. These designs have lowest mass and highest power densities. One optimal design from each optimization has been selected and plotted on the graph of active power density vs pole number. This graph is as shown in Fig. 4. As seen from Fig.4 the optimal design at 20 A/mm² occurs at 28-pole count and achievable maximum power density (considering active weight only) at this pole count from the slotless machine is 6.93 kW/kg. Similarly, at 30 A/mm² the optimal design occurs at 34 and 36-pole count and at this pole count maximum achievable active power density is 9.39 kW/kg. After the optimal point, the design reaches the

upper limit of the stator bore diameter i.e. 300 mm and further it increases length of the machine to achieve the constraint which results into higher mass and subsequently lower power densities. The design parameters are extracted from the analytical model and machine was designed in FEA software to check the validity. The validation of these designs has been performed by commercially available FEA software and results of which are shown in figures and graphs below.

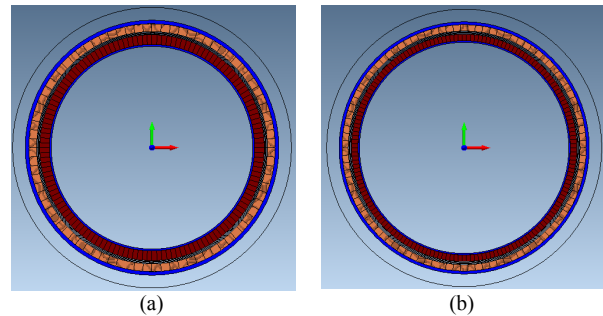


Fig. 7 Optimal and power dense design at (a) 42-Coils; 28-Poles machine at 20A/mm² and (b) 51-Coils; 34-Poles machine at 30A/mm²

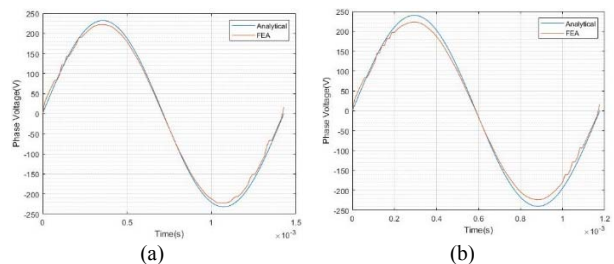


Fig. 8 Validation of analytical tool for back emf waveform for (a) 42-Coils; 28-Poles machine at 20A/mm² and (b) 51-Coils; 34-Poles machine at 30A/mm²

The average torque computation from FEA software and analytical tool is presented in the table below.

TABLE I
VALIDATION FOR FEA & ANALYTICALLY CALCULATED TORQUE

Cases	Average FEA Torque (Nm)	Average Analytical Torque (Nm)	% Variation
42C-28P; Current Density = 20A/mm ²	1580	1600	-1.25%
51C-34P; Current Density = 30A/mm ²	1510	1600	-5.625%

The design details of two optimal design at different current density is shown in Table II.

Table II
DESIGN PARAMETERS FOR OPTIMAL DESIGNS

	At 20 A/mm ²	At 30 A/mm ²	
Torque	1600	1600	Nm
Power	502.65	502.65	kW
Speed	3000	3000	rpm
Current Density	20.49	30.45	A/mm ²
Copper fill factor	0.6	0.6	-
Current	1443.5	1396	A
Turns	1	1	-
Peak Phase Back-EMF	235.19	243.235	V
Outer-most Diameter	328.41	321.1034	mm
Stator bore diameter	298.95	297.37	mm
Coil thickness	10.16	8.1207	mm
PM thickness	12.64	8.5	mm
Length	358.74	356.8421	mm
Stator yoke thickness	4.6	3.7	mm
Strand Area	70.44	45.85	mm ²
Lamination mass	19.07	15.4	Kg
Magnet mass	32.9	22.15	kg
Copper mass (active)	18.2	14.5	kg
End winding mass	2.4	1.5	kg
Total active weight	72.57	53.55	kg
Active Power Density	6.93	9.39	kW/kg

V. CONCLUSIONS

Earlier detailed research on slotted PM machine and its kW/kg for a similar power/speed showed a power density of 9.2kW/kg based on active mass and 5kW/kg based on the total mass [2]. This paper shows that with appropriate optimization and intensive cooling similar power density (based on active mass) is achievable with slotless machines. In follow-on work the authors will research in detail the mechanical, thermal, and passive component design optimization for the slotless PM machine to

establish a fairer power density comparison to the slotted machine based on the total mass.

REFERENCES

- [1] D. Golovanov, L. Papini, D. Gerada, Z. Xu, and C. Gerada, "Multidomain Optimization of High-Power-Density PM Electrical Machines for System Architecture Selection," *IEEE Trans. Ind. Electron.*, vol. 65, no. 7, pp. 5302–5312, 2018.
- [2] D. Golovanov, D. Gerada, Z. Xu, C. Gerada, A. Page, and T. Sawata, "Designing an advanced electrical motor for propulsion of electric aircraft," *AIAA Propuls. Energy Forum Expo. 2019*, no. August, 2019.
- [3] Z. P. Xia, Z. Q. Zhu, and D. Howe, "Analytical magnetic field analysis of halbach magnetized permanent-magnet machines," *IEEE Trans. Magn.*, vol. 40, no. 4 I, pp. 1864–1872, 2004.
- [4] A. Rahideh and T. Korakianitis, "Analytical magnetic field distribution of slotless brushless PM motors. Part 2: Open-circuit field and torque calculations," *IET Electr. Power Appl.*, vol. 6, no. 9, pp. 639–651, 2012.
- [5] Z. Song, C. Liu, and H. Zhao, "Comparative Analysis of Slotless and Coreless Permanent Magnet Synchronous Machines for Electric Aircraft Propulsion," *2019 22nd Int. Conf. Electr. Mach. Syst. ICEMS 2019*, 2019.
- [6] O. Wallmark and P. Kjellqvist, "Analysis of a low-cost air-gap winding for permanent magnet synchronous motors," *IEEE Trans. Energy Convers.*, vol. 24, no. 4, pp. 841–847, 2009.
- [7] SIEMENS AG, MUNICH, GERMANY, "Siemens develops world-record electric motor for aircraft" Mar 2015. [Online] Available: <https://press.siemens.com/global/en/pressrelease/siemens-develops-world-record-electric-motor-aircraft>